Computational Materials Science 46 (2009) 115–123

Contents lists available at ScienceDirect

Computational Materials Science

journal homepage: www.elsevier.com/locate/commatsci

Fatigue crack growth predictions based on damage accumulation calculations ahead of the crack tip

Jaime Tupiassú Pinho de Castro, Marco Antonio Meggiolaro *, Antonio Carlos de Oliveira Miranda

Mechanical Engineering Department, Pontifical Catholic University of Rio de Janeiro, Rua Marquês de São Vicente 225, Rio de Janeiro, RJ 22453-900, Brazil

ARTICLE INFO

Article history:
Received 5 November 2007
Received in revised form 9 February 2009
Accepted 10 February 2009

PACS:
62.20.Mk
62.20.Dc
62.20.Fe

Keywords:
Fatigue
Crack growth modeling
Critical damage model
Strain-life method
Hutchinson–Rice–Rosengren field
Crack growth algorithm

ABSTRACT

Models are proposed to predict the fatigue crack growth (FCG) process using crack initiation properties and critical damage concepts. The crack is modeled as a sharp notch with a very small but finite tip radius to remove its singularity, using a strain concentration rule. In this way, the damage caused by each load cycle and the effects of residual stresses can be calculated at each element ahead of the crack tip using the hysteresis loops caused by the loading, without the need for adjustable parameters. A computational algorithm is introduced to calculate cycle-by-cycle crack growth using the proposed methodology. A quite good agreement between the εN-based crack growth predictions and experiments is obtained both for constant and for variable amplitude load histories.

1. Introduction

Since the pioneer work of Majumdar and Morrow in 1974 [1], several models have been proposed to correlate the oligocyclic fatigue crack initiation process (controlled by the strain range $\Delta\varepsilon$) with fatigue crack propagation rates (controlled by the stress intensity range ΔK). Some of this so-called critical damage models consider the width of the volume element (VE) in the crack propagation direction as being the distance that the fatigue crack propagates on each cycle *da*. Others consider the fatigue crack propagation rate as being the VE width divided by the number of cycles that the crack would need to cross it.

However, most models do not properly deal with the supposed stress field singularity at the crack tip. This singularity implies that all the damage would be caused by the last loading event. Recently, an improved model that deals with the actual elastic–plastic stresses at the crack tip has been proposed [2]. It uses εN parameters and expressions of the HRR type to represent the elastic–plastic strain range inside the plastic zone ahead of the crack tip. The crack tip is modeled as a sharp notch with a very small but finite tip radius to remove the singularity issues. The origin of the HRR field is shifted from the crack tip to a point inside the crack, located by matching the HRR strain at the blunt crack tip with the strain predicted at that point by a strain concentration rule.

This non-singular model considers that the damage zone ahead of the crack tip is composed by a sequence of very small VE, each one loaded by a different strain range, which are broken sequentially as the crack propagates. Each of these VE will be submitted to elastic–plastic hysteresis loops of increasing amplitude as the crack tip approaches it (Fig. 1), even in the case of constant amplitude loading. Thus any given VE suffers damage during each load cycle, caused by the amplitude of the hysteresis loop acting in that cycle, which in turn depends on the distance r_i between the *i*th VE and the fatigue crack tip. Fracturing of the VE at the crack tip (which causes the fatigue crack growth) occurs when its accumulated damage reaches a critical value, due to the summation of the damage suffered during each cycle, quantified by a damage accumulation model.

In order to generalize the above idea to the variable amplitude (VA) loading case, it is necessary to perform cycle-by-cycle sequential calculations to be able to account for load sequence effects [3–6]. These effects, caused by several mechanisms that can retard or

* Corresponding author. Tel.: +55 21 35271424; fax: +55 21 35271165.
E-mail addresses: jtcastro@puc-rio.br (J.T.P. de Castro), meggi@puc-rio.br (M.A. Meggiolaro), amiranda@tecgraf.puc-rio.br (Antonio Carlos de Oliveira Miranda).

0927-0256/$ - see front matter © 2009 Elsevier B.V. All rights reserved.
doi:10.1016/j.commatsci.2009.02.012

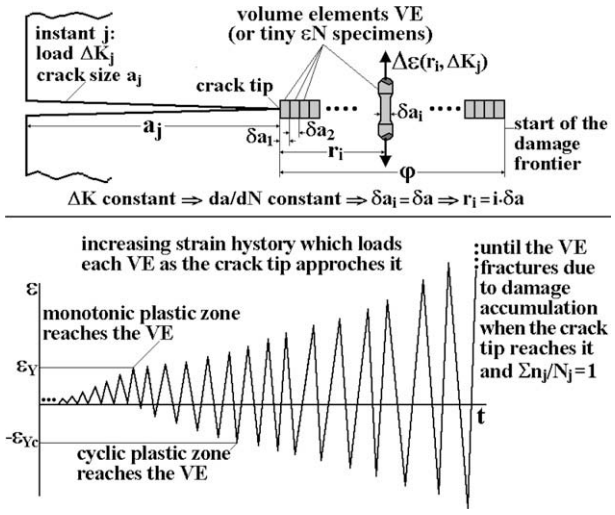

Fig. 1. Schematics of the FCG assumed to be caused by the sequential fracture of volume elements (or tiny εN specimens) at every load cycle, loaded by an increasing strain history as the crack tip approaches them.

accelerate the growth of a fatigue crack after significant load amplitude variations, are very significant and must be considered. These load interaction mechanisms can act *behind*, *at* or *ahead* of the crack tip. Among them, it is important to mention: (i) crack closure, acting *behind* the crack tip, which can be caused by plasticity, oxidation or roughness of the crack faces, or even by strain induced phase transformation; (ii) crack tip blunting, kinking or bifurcation, acting *at* or close to the crack tip; and (iii) residual stress and strain fields, which act *ahead* of the crack tip.

Most load sequence effects models in fatigue crack growth (FCG) are still based on Elber's plasticity-induced crack closure. However, there are several important problems that cannot be explained by Elber's effective stress intensity range ΔK_{eff} concept. For example, a strong objection against crack closure is based on convincing experimental evidence such as fatigue crack growth threshold values ΔK_{th} that are higher in vacuum than in air [7]. Another very important problem that cannot be explained by the Elber mechanism is crack delay or arrest after overloads under high $R = K_{min}/K_{max}$ ratios, when the minimum value K_{min} of the applied stress intensity range $\Delta K = K_{max} - K_{min}$ always remains *above* K_{op}, the (measured) load that opens the fatigue crack [8]. In this case, there is no closure either before or after the overloads.

In this work, the idea that FCG is caused by the sequential failure of VE ahead of the crack tip is extended to deal with the VA loading case, using a non-singular damage model. A cycle-by-cycle computational algorithm is proposed, to be able to calculate the variable crack increments at each cycle and to account for load sequence effects. The methodology not only explicitly considers the mechanisms acting *ahead* of the crack tip, but it is also able to include effects of the mechanisms acting *behind* it such as crack closure. The methodology is described next.

2. The non-singular damage model

The damage *ahead* of a fatigue crack tip can be estimated using simple but sound hypotheses and standard fatigue calculations, supposing that fatigue cracks grow by sequentially breaking small volume elements (VE) ahead of their tips, which fracture when the crack tip reaches them because they accumulated all the damage the material can support. In this way, εN procedures can be combined with fracture mechanics concepts to *predict* FCG, using the cyclic properties of the material and the strain distribution ahead of the crack tip. These models can consider the VE width in the FCG direction as being the distance that the crack grows during each cycle, or the FCG rate as being the VE width divided by the number of cycles that the crack would need to cross it.

Critical damage models are not new [1,9–12], but they still need improvements. Most models assume singular stress and strain fields ahead of the crack tip (concentrating in this way all the damage very next to the tip), and thus need some adjustable constant to fit the FCG *da/dN* data, irreversibly compromising their *prediction* potential in this way. However, the supposed singularity at the crack tip is a characteristic of the mathematical models that postulate a zero radius tip, not of the real cracks, which have a blunt tip when loaded. In other words, real cracks must have finite strains at their tip under load, or else they would be unstable. To avoid this problem, the actual finite strain range at the crack tip $\Delta\varepsilon_{tip}$ can be estimated using the stress concentration factor K_t for the blunt crack [13] and a strain concentration rule. The strain range field ahead of the crack tip can then be upper-bounded by $\Delta\varepsilon_{tip}$, e.g. by assuming $\Delta\varepsilon_{tip}$ constant where the singular solution would predict strains greater than $\Delta\varepsilon_{tip}$, or by translating the singular strain field, as discussed later.

A few models assume that the entire fatigue damage occurs inside a small region next to the crack tip. They use the number of cycles N^* associated with $\Delta\varepsilon_{tip}$ (which can be obtained from Coffin–Manson's equation, e.g.) to calculate the FCG rate as the length of this region divided by N^*. But such models have two shortcomings. First, neglecting the fatigue damage beyond this region concentrates it in the very last N^* cycles, a non-conservative hypothesis. Second, assuming intermittent and not a cycle-by-cycle fatigue-induced increments in the crack length, although valid in some cases of crazing in polymers, is certainly not true for most metallic structures, as evidenced by their striated crack surfaces.

Kujawski and Ellyin [11] proposed a model to relate fatigue crack initiation and propagation with the plastic work per cycle, which can be used to treat cumulative damage problems. In another work [12], the same authors joined low-cycle fatigue properties and stress/strain field equations to model *R*-ratio effects on fatigue crack growth curves, assuming that the fatigue failure criterion within the process zone was the plastic strain energy density. They used a solution for the stress and strain distribution ahead of the crack tip based on Rice's analytical solution for mode III under small scale yielding, adapted to mode I based on McClintock's analogy between modes III and I. However, the resulting distribution is singular. To solve this issue, they have used a process zone size δ^*, immediately ahead of the crack tip. The resulting model correlated well with experiments, however the limitations of assuming the existence of the process zone size δ^*, beyond which the damage could be neglected, are the same as the ones from the models that use N^*, described above.

To avoid these limitations, the model proposed in this work uses Schwalbe's modification [9] of the HRR field to represent the strain range distribution ahead of the crack tip. Then, it removes the crack tip singularity by shifting the origin of the strain field from the crack tip to a point inside the crack, located by matching the crack tip strain with $\Delta\varepsilon_{tip}$ predicted by a strain concentration rule, such as Neuber [14], Molsky–Glinka [15], or the linear rule [16]. This approach recognizes that the strain range $\Delta\varepsilon(r_i, \Delta K)$ in all unbroken VE increases and causes damage during each load cycle as the crack tip approaches them, see Fig. 1. Therefore, the VE closest to the tip breaks due to the summation of the damage induced by all previous load cycles (which under constant amplitude load increases as r_i decreases while the crack grows), and not only by the damage induced in the very last load cycle. In this way, the fatigue crack growth rate under constant ΔK can be modeled by the sequential failure of identical VE ahead of the crack tip.

This model is then extended to deal with the variable amplitude loading case, which has idiosyncrasies that must be treated appropriately. First, the VE that breaks in any given cycle must have variable width, which should be calculated by locating the point ahead of the crack tip where the accumulated damage reaches a specified value. Note that there are limitations with the use of the Palmgreen–Miner linear damage law, as pointed out in [11]. This is because cycling sequences from a low to a high stress level can result in crack initiation with an accumulated linear damage larger than one, while sequences from high to low can initiate a crack with values lower than one. However, since there is no a priori information on the loading order, in this paper the Palmgreen–Miner model is used, defining as 1.0 the critical damage value.

Load sequence effects, such as overload-induced crack growth retardation, are associated with mean load effects caused by elastic–plastic hysteresis loop shifts, and can be calculated using the powerful numerical tools available in the *ViDa* software [17]. Moreover, this model can recognize an opening load, and thus can separate the cyclic damage from the closure contributions to the crack growth process. The necessary equations for constant and variable amplitude loadings are discussed next.

3. Constant amplitude loading

In every load cycle, each VE ahead of the crack tip suffers strain loops of increasing range as the tip approaches it, and a damage increment that depends on the strain range in that cycle, thus on r_i (the distance from the ith VE to the tip) and on the load ΔK_j at that event. The fracture of the VE at the crack tip occurs because it accumulated its critical damage, e.g. by Miner's rule when $\sum n_j/N_j = 1$, where n_j is the number of cycles of the jth load event and N_j is the number of cycles that the piece would last if loaded solely by that event's loading levels. If under constant ΔK (or ΔK_{eff}) the fatigue crack advances a fixed distance δa in every load cycle, and if, for simplicity, the damage outside the cyclic plastic zone zp_c is neglected, there are thus $zp_c/\delta a$ VE ahead of the crack tip at any instant that need to be considered. Since the plastic zone advances with the crack, each new load cycle breaks the VE adjacent to the crack tip, induces an increased strain range in all other unbroken VE, and adds a new element to the damage zone, thus $n_j = 1$. Moreover, since the VE are considered as small εN specimens, they break when:

$$\sum_{i=0}^{zp_c/\delta a} \frac{1}{N(zp_c - i\cdot\delta a)} = \sum_{r_i=0}^{zp_c} \frac{1}{N(r_i)} = 1 \tag{1}$$

where $N(r_i) = N(zp_c - i\cdot\delta a)$ is the fatigue life corresponding to the plastic strain range $\Delta\varepsilon_p(r_i)$ acting at a distance r_i from the crack tip. This fatigue life can be calculated using the plastic part of Coffin–Manson's rule

$$N(r_i) = \frac{1}{2}\left(\frac{\Delta\varepsilon_p(r_i)}{2\varepsilon_c}\right)^{1/c} \tag{2}$$

where ε_c and c are the plastic coefficient and exponent, and $\Delta\varepsilon_p(r_i)$ in its turn can be described by Schwalbe's [9] modification of the HRR field

$$\Delta\varepsilon_p(r_i) = \frac{2S_{Yc}}{E}\cdot\left(\frac{zp_c}{r_i}\right)^{\frac{1}{1+h_c}} \tag{3}$$

where S_{Yc} is the cyclic yield strength, h_c is the Ramberg–Osgood cyclic hardening exponent, and zp_c is the cyclic plastic zone size in plane strain, which, if v is Poisson's coefficient, can be estimated by

$$zp_c = \frac{(1-2v)^2}{4\pi\cdot(1+h_c)}\cdot\left(\frac{\Delta K}{S_{Yc}}\right)^2 \Rightarrow N(r_i) = \frac{1}{2}\left[\frac{S_{Yc}}{E\varepsilon_c}\cdot\left(\frac{zp_c}{r_i}\right)^{\frac{1}{1+h_c}}\right]^{1/c} \tag{4}$$

The HRR field describes the plastic strains ahead of an idealized crack tip, thus it is singular at $r_i = 0$. But an infinite strain is physically impossible. This does not mean that singular models are useless, but only that the damage close to the crack tip is not predictable by them. To eliminate this unrealistic strain singularity, the origin of the HRR coordinate system is shifted into the crack by a small distance X, copying Creager and Paris' idea [13]. Approximating Miner's summation by an integral, setting the VE width δa equal to an infinitesimal da at a distance dr ahead of the crack tip, which is easier to deal with [2], then

$$\Delta\varepsilon_p(r+X) = \frac{2S_{Yc}}{E}\cdot\left(\frac{zp_c}{r+X}\right)^{\frac{1}{1+h_c}} \tag{5}$$

$$\frac{da}{dN} = \int_0^{zp_c}\frac{dr}{N(r+X)} \tag{6}$$

To determine X and $N(r+X)$, two different paths can be followed. The first uses Creager and Paris' offset $X = \rho/2$, where ρ is the actual crack tip radius estimated by $\rho = \mathrm{CTOD}/2$, thus

$$X = \frac{\rho}{2} = \frac{\mathrm{CTOD}}{4} = \frac{K_{\max}^2\cdot(1-2v)}{\pi\cdot E\cdot S_{Yc}}\cdot\sqrt{\frac{1}{2(1+h_c)}} \tag{7}$$

Note that the effect of K_{max} is taken into account using the above equation, where the CTOD does not depend on the load history and associated residual stresses. This is a limitation from such first path to solve the singularity issue.

The second path is more reasonable. Instead of arbitrating the offset of the strain field origin, X is determined by first calculating the crack linear elastic stress concentration factor K_t [13]

$$K_t = 2\Delta K/(\Delta\sigma_n\cdot\sqrt{\pi\rho}) \tag{8}$$

For any given ΔK and R, it is possible to calculate ρ and K_t from Eqs. (7) and (8), and then the stress and strain ranges $\Delta\sigma_{tip}$ and $\Delta\varepsilon_{tip}$ at the crack tip using a strain concentration rule. Assuming that the material stress–strain behavior is parabolic, with cyclic strain hardening coefficient H_c and exponent h_c, and neglecting the elastic range, the Linear, Neuber and Molsky–Glinka concentration rules give, respectively

$$\Delta\varepsilon_{tip} = \frac{K_t\cdot\Delta\sigma_n}{E} = \frac{2\Delta K}{E\sqrt{\pi\cdot\mathrm{CTOD}/2}} \tag{9}$$

$$\begin{cases} \Delta\sigma_{tip}\cdot\Delta\varepsilon_{tip} = \frac{(K_t\Delta\sigma_n)^2}{E} = \frac{8\Delta K^2}{E\cdot\pi\cdot\mathrm{CTOD}} \\ \Delta\varepsilon_{tip} = 2\left(\frac{\Delta\sigma_{tip}}{2H_c}\right)^{1/h_c} \end{cases} \tag{10}$$

$$\begin{cases} \frac{2\Delta K^2}{E\cdot\pi\cdot CTOD} = \frac{\Delta\sigma_{tip}^2}{4E} + \frac{\Delta\sigma_{tip}}{1+h_c}\cdot\left(\frac{\Delta\sigma_{tip}}{2H_c}\right)^{1/h_c} \\ \Delta\varepsilon_{tip} = 2\left(\frac{\Delta\sigma_{tip}}{2H_c}\right)^{1/h_c} \end{cases} \tag{11}$$

After calculating $\Delta\varepsilon_{tip}$ at the crack tip using one of these rules, the shift X of the HRR origin is obtained by

$$\Delta\varepsilon_{tip} = \frac{2S_{Yc}}{E}\cdot\left(\frac{zp_c}{X}\right)^{\frac{1}{1+h_c}} \Rightarrow X = zp_c\cdot\left(\frac{2S_{Yc}}{E\Delta\varepsilon_{tip}}\right)^{1+h_c} \tag{12}$$

The strain distribution at a distance r ahead of the crack tip, $\Delta\varepsilon_p(r+X)$, without the singularity problem at the crack tip, can now be readily obtained by

$$\frac{da}{dN} = \int_0^{zp_c} 2\cdot\left(\frac{2\varepsilon_c}{\Delta\varepsilon_p(r+X)}\right)^{1/c} dr \tag{13}$$

This prediction is experimentally verified in SAE 1020 and API 5L X-60 steels and in a 7075 T6 aluminum alloy, using Eq. (13) to obtain the constant of a McEvily-type da/dN equation, which describes the $da/dN \times \Delta K$ curves using only one adjustable parameter A,

$$\frac{da}{dN} = A[\Delta K - \Delta K_{th}(R)]^2 \left(\frac{K_c}{K_c - [\Delta K/(1-R)]}\right) \tag{14}$$

where K_c and $\Delta K_{th}(R)$ are the material fracture toughness and crack propagation threshold at the load ratio R. For the experimental verification, the values of K_c, $\Delta K_{th}(R)$ and the εN and da/dN data are all obtained by testing proper specimens manufactured from the same stock of the three materials, following ASTM standards. The API 5L X-60 $da/dN \times \Delta K$ experimental curves are compared with this simple model predictions in Fig. 2. Both the shape and the magnitude of the data are quite reasonably reproduced by this critical damage model. The Linear rule generates better *predictions* probably because the tests are performed under predominantly plane strain conditions. Moreover, since this model does *not* use any adjustable constant, this performance is certainly no coincidence. The Linear rule also results in good predictions for the SAE 1020 steel and 7075 T6 aluminum [2].

Despite this encouraging performance, a few remarks are still required. First, the damage beyond zp_c has been neglected to simplify the numerical calculations. This hypothesis is non-conservative, because there is significant damage beyond zp_c, as it will be shown later. Instead, the monotonic plastic zone border zp will be considered in this simplification. Second, FE calculations [18] indicate that there is a region adjacent to the blunt crack tip with a strain gradient much lower than predicted by the HRR field. These problems can be avoided by shifting the origin *away* from the tip by a distance x_2 and assuming the crack tip strain range $\Delta\varepsilon_{tip}$ constant over the region I of length $x_1 + x_2$, shown in Fig. 3. The value of x_1 can be obtained equating $\Delta\varepsilon_{tip}$ and the HRR-calculated strain range, and from the crack tip stress range $\Delta\sigma_{tip}$

$$\Delta\sigma_{tip} = \Delta\sigma(r = x_1) = 2S_{Yc} \cdot \left(\frac{zp_c}{x_1}\right)^{\frac{h_c}{1+h_c}} = 2S_{Yc} \cdot \left(\frac{E \cdot \Delta\varepsilon_{tip}}{2S_{Yc}}\right)^{h_c} \tag{15}$$

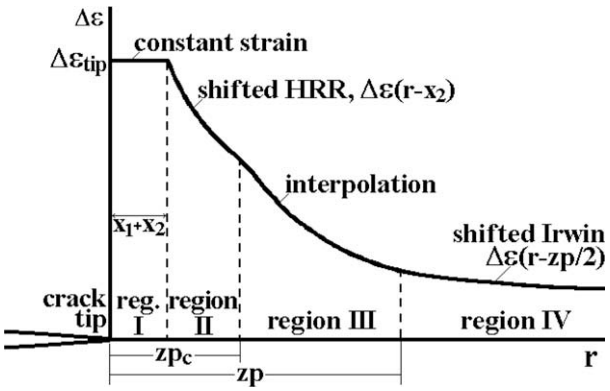

Fig. 3. Proposed strain range distribution, divided in four regions to consider both the elastic and the plastic contributions to the damage ahead of the crack tip.

Then, following Irwin's classical idea, the value of the shift x_2 is obtained by integrating the stress field $\sigma(r)$, enforcing equilibrium of the applied force

$$\int_0^{\infty} \Delta\sigma(r)dr = \int_0^{x_1+x_2} \Delta\sigma_{tip}dr + \int_{x_1}^{\infty} \Delta\sigma(r)dr \Rightarrow \int_0^{x_1} \Delta\sigma(r)dr = \int_0^{x_1+x_2} \Delta\sigma_{tip}dr \tag{16}$$

Since $x_1 < zp_c$, $\Delta\sigma(r)$ in the above integral can still be described by the HRR solution, resulting in

$$\int_0^{x_1} 2S_{Yc} \cdot \left(\frac{zp_c}{r}\right)^{\frac{h_c}{1+h_c}} dr = \Delta\sigma_{tip} \cdot x_1 \cdot (1+h_c) = \Delta\sigma_{tip} \cdot (x_1 + x_2) \Rightarrow x_2 = x_1 \cdot h_c \tag{17}$$

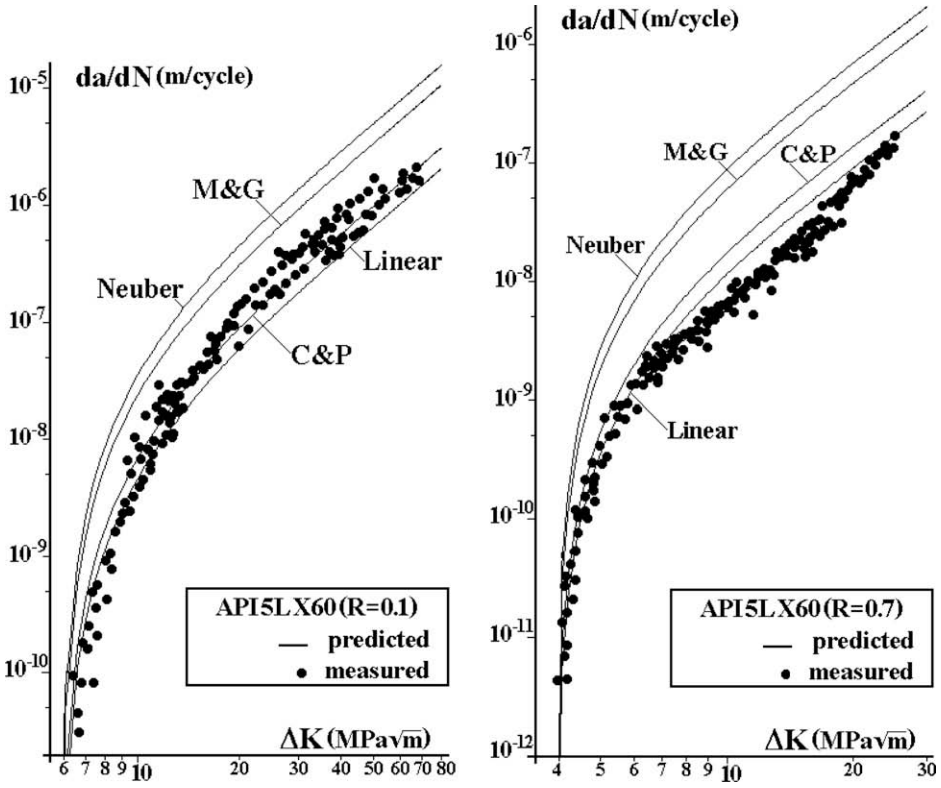

Fig. 2. $da/dN \times \Delta K$ behavior measured and *predicted* by the various strain concentration rules used in the critical damage model, for API-5L-X60 pipeline steel at $R = 0.1$ and $R = 0.7$ [2].

These simple tricks generate a more reasonable strain distribution model, see Fig. 3:

$$\Delta\varepsilon(r) = \Delta\varepsilon_{tip},\ 0 \leqslant r \leqslant x_1 + x_2 \text{ (region I)} \tag{18}$$

$$\Delta\varepsilon(r) = \frac{2S_{Yc}}{E}\cdot\left(\frac{zp_c}{r - x_2}\right)^{\frac{1}{1+h_c}},\ x_1 + x_2 < r \leqslant zp_c + x_2 \text{ (region II, shifted HRR)} \tag{19}$$

$$\Delta\varepsilon(r) \cong \frac{2S_{Yc}}{E}\cdot\sqrt{\frac{zp_c + x_2}{r}}\cdot\left(1 + v\frac{r - zp_c}{zp - zp_c}\right),\ zp_c + x_2 < r < zp \text{ (region III)} \tag{20}$$

$$\Delta\varepsilon(r) = \frac{\Delta K\cdot(1+v)}{\kappa E\sqrt{2\pi(r - zp/2)}},\ r \geqslant zp \text{ (region IV, shifted Irwin)} \tag{21}$$

where $\kappa = 1$ for plane stress and $\kappa = 1/(1-2v)$ for plane strain, and

$$zp = \frac{1}{\pi\kappa^2}\cdot\left(\frac{K_{\max}}{S_{Yc}}\right)^2 \text{ and } zp_c = \frac{1}{4\pi\kappa^2\cdot(1+h_c)}\cdot\left(\frac{\Delta K}{S_{Yc}}\right)^2 \tag{22}$$

Both constant (CA) and variable amplitude (VA) FCG can then be calculated using Eqs. (18)–(22), which consider all the damage ahead of the crack tip and provide a more realistic model of the FCG process. But Eqs. (2), (5) and (13) must be modified to include elastic parameters σ_c and b, and to account for the mean load σ_m effects on the VE life using Morrow elastic, Morrow elastic–plastic or Smith–Watson–Topper equations. But the life N in these equations cannot be explicitly written as a function of the VE strain range and mean load and thus must be calculated numerically, a programming task that, despite introducing no major conceptual difficulty, is far from trivial, as discussed in the next sections.

4. Variable amplitude loading

The $da/dN \times \Delta K$ curve predicted for CA loads could be used with a FCG load interaction model to treat VA problems [19]. But the idea here is to *directly* quantify the fatigue damage induced by the VA load considering the crack growth as caused by the sequential fracture of *variable* size VE ahead of the crack tip. Since the Linear strain concentration rule generated better predictions above, it is the only one used here. Because load interaction effects can have a significant importance in FCG, they are modeled by using Morrow elastic equation to describe the VE fatigue life N

$$N(r+X) = \frac{1}{2}\left(\frac{\Delta\varepsilon_p(r+X)}{2\varepsilon_c}\left(1 - \frac{\sigma_m}{\sigma_c}\right)^{-c/b}\right)^{1/c} \tag{23}$$

To account for mean load effects, a modified stress intensity range can be easily implemented for $R > 0$ to filter the loading cycles that cause no damage by using

$$\Delta K_{eff} = K_{\max} - K_{PR} = \frac{\Delta K}{1-R} - K_{PR} \tag{24}$$

where K_{PR} is a propagation threshold that depends on the considered retardation mechanism, such as K_{op} from Elber's equation [20] or K^*_{max} from the Unified Approach [7]. The damage function for each cycle is then

$$d_i(r + X_i) = \frac{n_i}{N_i(r + X_i)} \tag{25}$$

If the material ahead of the crack is supposed virgin, then its increment δa_1 caused by the first load event is the value $r = r_1$ that makes Eq. (25) equal to one, therefore

$$d_1(r_1 + X_1) = 1 \Rightarrow \delta a_1 = r_1 \tag{26}$$

In all subsequent events, the crack increments must also account for the damage accumulated by the previous loadings, in the same way as it was done for the constant loading case. But as the coordinate system moves with the crack, a coordinate transformation of the damage functions is necessary:

$$D_i = \sum_{j=1}^{i} d_j\left(r + \sum_{p=j}^{i-1}\delta a_p\right) \tag{27}$$

Since the distance $r = r_i$ where the accumulated damage equals one in the ith event is a variable that depends on ΔK_i (or ΔK_{effi}) and on the previous loading history, VE of different widths may be bro-

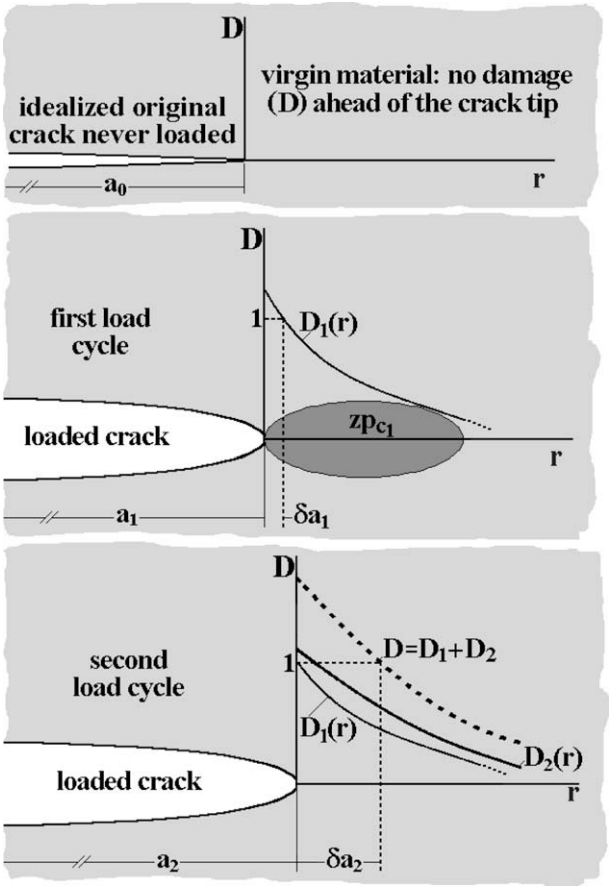

Fig. 4. Schematics of the critical damage calculations, which under variable amplitude loading recognize variable crack increments by forcing the crack to grow over the region where the accumulated damage $D = 1$.

ken at the crack tip by this model. This idea is illustrated in Fig. 4. In the next section, an algorithm is proposed to computationally implement the above methodology.

5. Simulation algorithm

The proposed algorithm to numerically calculate fatigue crack growth under VA loading from the presented critical damage model is described here. Note that, naturally, CA loadings can also be calculated using this algorithm.

Instead of using variable width volume elements, which would be difficult to handle computationally since such widths are not known *a priori*, the algorithm assumes that all VE have constant width δa. However, it allows the existence of a partially cracked VE at the crack tip, with residual ligament rl. The idea behind the calculations is to find at each cycle the number of fractured VE and the new value of rl, obtaining then the crack increment. The algorithm equations are described next.

First, upper bounds to the obtainable monotonic and cyclic yield zones are calculated. If the maximum values of K_{max} and ΔK throughout the entire history are known, respectively $\max(K_{max})$ and $\max(\Delta K)$, then the upper bounds result in

$$zp_{max} = \frac{1}{\pi\kappa^2}\cdot\left(\frac{\max(K_{max})}{S_{Yc}}\right)^2 \text{ and } zp_{c,max} = \frac{1}{4\pi\kappa^2\cdot(1+h_c)}\cdot\left(\frac{\max(\Delta K)}{S_{Yc}}\right)^2 \quad (28)$$

If these maximum values are not known *a priori*, then they can be conservatively replaced by the fracture strength K_c in the above equations.

The simulation resolution is set by the constant width δa of the VE, which is chosen in this work as 10^{-7} m. To reduce the memory requirements and speed up the algorithm, only a domain of length Δa ahead of the crack tip is considered, i.e. the damage at the volume elements beyond this distance is neglected. Traditional critical damage models consider this domain Δa equal to the size of the current cyclic yield zone. However, this may lead to non-conservative errors because the plastic deformation between the monotonic and cyclic yield zones also contributes to significant accumulated damage. As seen in the hysteresis loops of a VE under constant ΔK loading (Fig. 5), the accumulated damage is already 0.47 in this example when the VE is reached by the cyclic plastic zone border. Neglecting this damage caused exclusively by the monotonic plastic zone would lead to non-conservative errors of almost 100% in the crack growth rate estimates. But in general it is not necessary to evaluate the damage at VE beyond the monotonic zone zp, as seen in Fig. 5, where the accumulated damage would still be very close to zero.

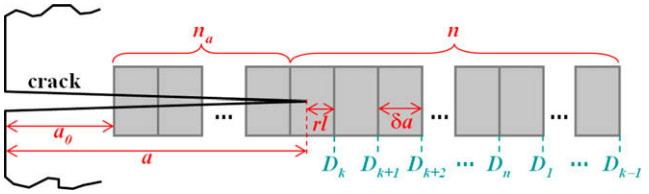

Fig. 6. Volume elements before and ahead of the crack tip, showing the main length parameters and the locations for the calculation of the accumulated damages D_1 through D_n.

In this work, two domain sizes Δa are considered, either zp_{max} or $zp_{c,max}$. Note that these domains are already overestimated, since they use the upper bounds of zp or zp_c, and not their values at each loading. This guarantees that the size of the calculation domain will be always larger than the monotonic or cyclic plastic zones independently of the loading history.

For a resolution δa and domain length Δa, the accumulated damage needs to be calculated at the borders of an integer number $n = \Delta a/\delta a$ of VE. This is accomplished by the n variables $D_1, D_2, \ldots, D_n$, see Fig. 6. Note in the figure that the integer variable k denotes the index of the variable D_k associated with the damage at the next border of the VE where the crack tip is currently located. These n damage variables form a cyclic set, meaning that the variable D_n will be followed by D_1, see Fig. 6.

In this algorithm, the current crack size a is represented as a function of the initial crack length a_0, an integer number n_a of already broken VE, and the residual ligament width rl in the partially cracked VE where the crack tip is currently located ($0 < rl \leqslant \delta a$, see Fig. 6), by

$$a = a_0 + n_a\cdot\delta a + (\delta a - rl) \quad (29)$$

In the beginning of the calculations, $rl = \delta a$ and $n_a = 0$, resulting in $a = a_0$ as expected. In addition, all damage variables are initially set to zero, and $k = 1$.

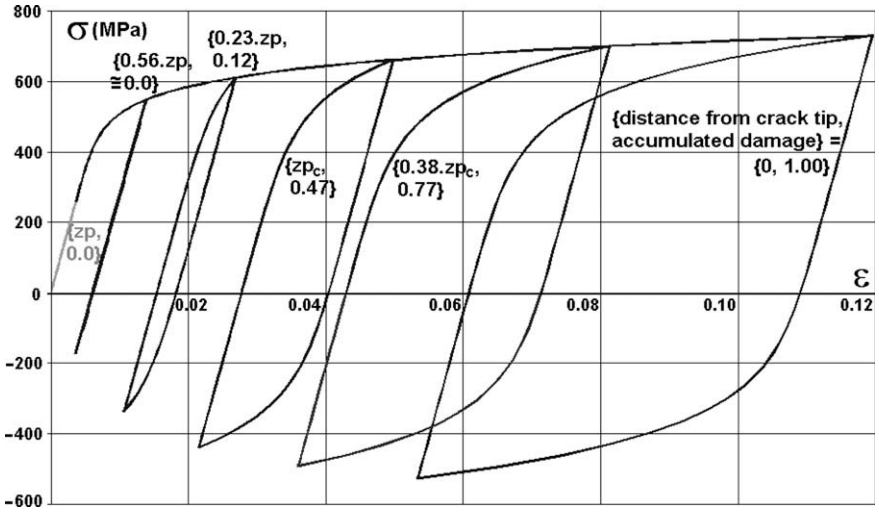

Fig. 5. Schematics of the hysteresis loops at a fixed VE at different crack growth stages, under constant ΔK loading, showing that an accumulated damage of 0.47 is already present in this VE when it is reached by the cyclic plastic zone zp_c.

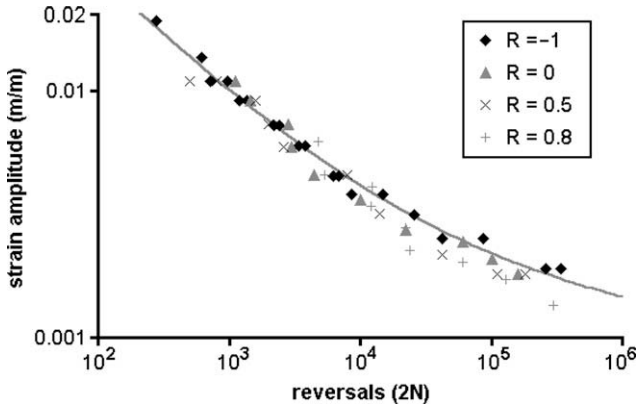

Fig. 7. Strain-life data for the API-5L-X52 steel, and Morrow elastic model that best fitted this data.

The applied loading is then counted using a sequential rain-flow algorithm [19] to preserve loading order. For each event, the alternate and mean nominal stresses are calculated, obtaining ΔK, $R = K_{min}/K_{max}$, and the current plastic zone sizes zp and zp_c. If ΔK is above the propagation threshold ΔK_{th}, which can indirectly include crack closure effects, then the damage at each VE is calculated.

The current CTOD and ρ are calculated from Eq. (7). The Eqs. (9)–(11) can then be used to obtain the crack tip stress and strain ranges, calculating the shift X of the HRR origin from Eq. (12).

Assuming that the damage caused by the current event can be neglected beyond the monotonic plastic zone, then at most the first i_{max} VE ahead of the crack tip need to be considered. Here, i_{max} is equal to $[\text{int}(zp/\delta a) + 2]$, where $\text{int}(x)$ is the function that returns the largest integer smaller than or equal to x. The distance r_i between the crack tip and the ith VE border beyond it, associated with the accumulated damage D_{k+i-1}, is

$$r_i = rl + (i-1)\cdot\delta a \tag{30}$$

The strain ranges $\Delta\varepsilon(r_i)$ and associated damage are then calculated from Eqs. (18)–(25) for $i = 1, 2, \ldots, i_{max}$. Such damage values at the VE borders are then added to the accumulated D_{k+i-1}.

Then, the largest index $i = i_b$ is found such that $D_{k+i_b-1} \geqslant 1$ (or greater than any other parameter defined using Miner's rule). If i_b exists, then i_b VE are broken at the current event, and i_b is added to the total number n_a of broken elements.

The new residual ligament rl in the first unbroken VE, to where the crack tip has advanced, is obtained from a linear interpolation between the accumulated damages at its borders:

$$rl = \delta a \cdot \frac{1 - D_{k+i_b}}{D_{k+i_b-1} - D_{k+i_b}} \tag{31}$$

The i_b broken VE do not need anymore the variables D_k through D_{k+i_b-1}, which are all reset to zero. Then, i_b new VE are created beyond the current domain border to keep the number of VE in the domain constant. The accumulated damage from these new VE will be stored in the just freed up variables D_k through D_{k+i_b-1}. Note that n_a can eventually become larger than n, because of the new VE generated each time the crack advances. Finally, the index k is increased by i_b, and the algorithm continues to evaluate the next event. It is easy to show that $k = (n_a \bmod n) + 1$, where $(x \bmod y)$ is equal to the remainder of the integer division between x and y. Note that if any index in the described algorithm results in a value i larger than n, then it is replaced by $(i \bmod n)$.

After all loadings have been sequentially considered in the calculations, the final crack size is evaluated using Eq. (29) and the final values of n_a and rl.

6. Experimental results

FCG tests under VA loading are performed on API-5L-X52 steel [21] 50 × 10 mm compact tension C(T) specimens, pre-cracked under CA at $\Delta K = 20$ MPa $\sqrt{m}$ until reaching crack sizes $a \cong 12.6$ mm. These cracks are measured with a 20 μm accuracy by optical methods and by a strain gage bonded at the back face of the specimens. The basic monotonic and cyclic properties, measured in computer-controlled servo-hydraulic machines using standard testing procedures, are $E = 200 \times 10^3$, $S_U = 527$, $S_Y = 430$, $S_{Yc} = 370$, $H_c = 840$ and $\sigma_c = 720$ (all in MPa), $h_c = 0.132$, $\varepsilon_c = 0.31$, $b = -0.076$ and $c = -0.53$, where σ_c and b are Coffin–Manson's elastic coefficient and exponent.

About 50 εN specimens are tested under deformation ratios varying from $R = -1$ to 0.8 (at least two specimens are tested at each strain range) to measure the mean load effect on the εN fatigue crack initiation curve, see Fig. 7. Morrow's strain-life equation, which includes the mean stress effect only in Coffin–Manson's elastic term, best fits the experimental data. The basic da/dN curve, measured using the same equipment, is well fitted by a modified Elber-type equation $da/dN(R = 0.1) = 2 \times 10^{-10}\ (\Delta K - 8)^{2.4}$ (da/dN in m/cycle and ΔK in MPa $\sqrt{m}$), using the crack propagation threshold $\Delta K_{th}(R = 0.1) = 8$ MPa $\sqrt{m}$ to replace K_{op}.

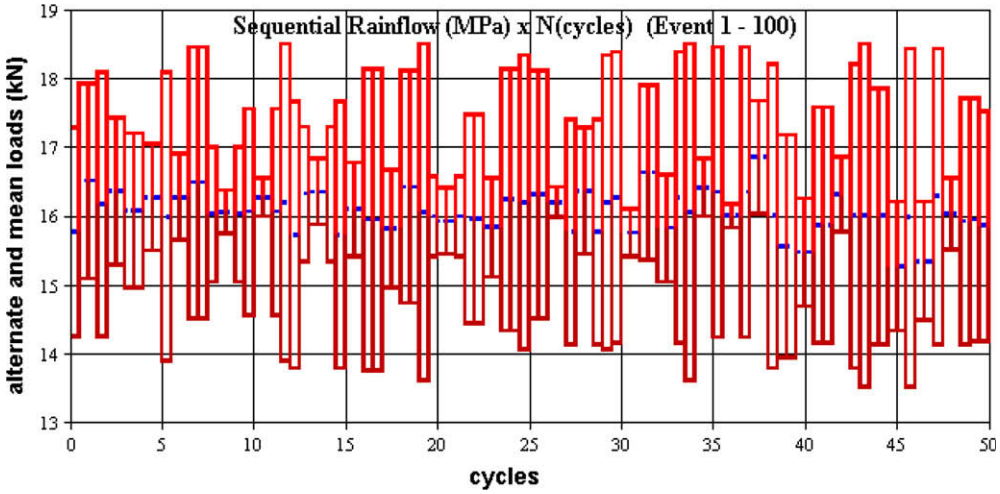

Fig. 8. Sequential rain-flow of the variable amplitude load block applied to the API-5L-X52 steel.

FCG tests are then conducted under a VA history with 50,000 blocks containing 100 reversals each. The load history is counted by the sequential rain-flow method, using the *ViDa* software [17]. The sequential rain-flow count of each applied block is shown in Fig. 8. Note the high mean stress levels, which have been chosen to avoid crack closure effects (the crack is always opened during such loading).

The damage calculation is made using a specially developed software code following the algorithm discussed above. The constant width δa of the VE is chosen as 10^{-7} m. Calculations with δa smaller than 10^{-7} m result in the same crack growth values within 0.1%. This means that in this case this resolution is enough to guarantee convergence.

Assuming that the maximum values of K_{max} and ΔK throughout the entire history are smaller than 20 MPa $\sqrt{m}$ (which could only be verified later, after the calculations), then Eq. (28) results in the upper bounds $zp_{max} = 0.127$ mm and $zp_{c,max} = 0.0281$ mm. The domain length $\Delta a = 0.127$ mm is used in this calculation, resulting in only $n = \Delta a/\delta a = 1274$ volume elements. Note that if the memory optimization method used in the proposed algorithm was not used, then a domain Δa of the size of the CTS residual ligament $50 - 12.6 = 37.4$ mm would require $n = 374{,}000$ volume elements instead.

The crack growth predictions based solely on εN parameters are quite reasonable, see Fig. 9. The prediction assuming no damage outside the cyclic plastic zone zp_c underestimated the crack growth. However, when the small (but significant) damage in the material between the cyclic and monotonic plastic zone borders is also included in the calculations, as described in the proposed

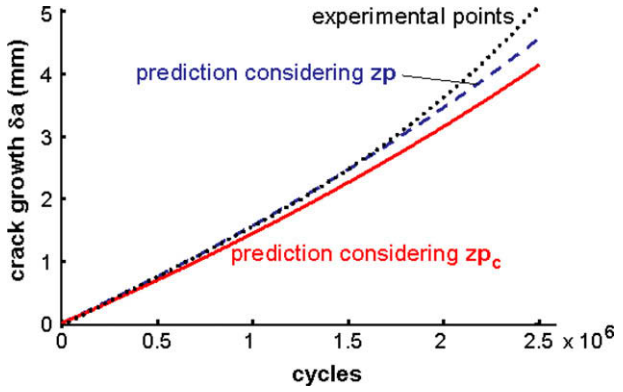

Fig. 9. Comparison between crack growth measurements and εN-based predictions for the variable amplitude load presented in Fig. 8 (API-5L-X52 steel).

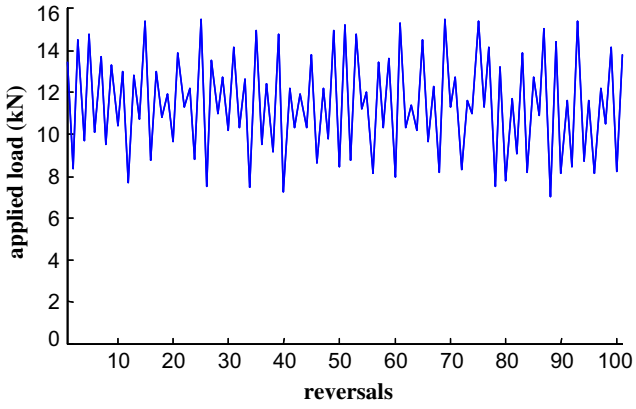

Fig. 10. VA load block applied to the SAE 1020 steel compact tension specimen.

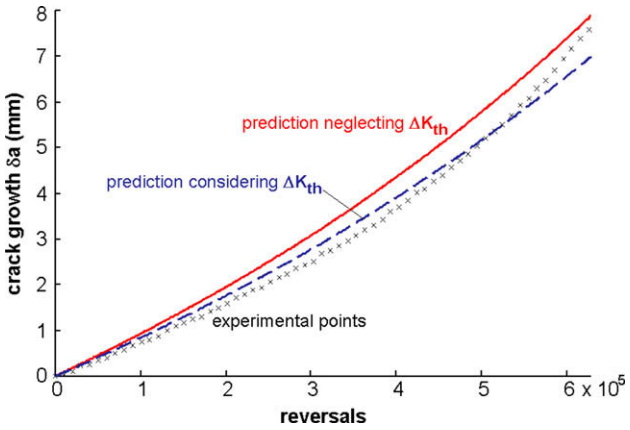

Fig. 11. Comparison between crack growth measurements and εN-based predictions for the variable amplitude load presented in Fig. 10 (SAE 1020 steel).

algorithm, an even better agreement is obtained. Note also that crack growth is slightly underestimated after 1.8×10^6 cycles, probably because these calculations neglected the (small) elastic damage and its mean stress effects.

A similar VA fatigue crack propagation test is conducted on compact tension C(T) specimens of SAE 1020 steel [22], with measured properties $E = 205$ GPa, $S_U = 491$, $S_Y = 285$, $S_{Yc} = 270$, $H_c = 941$ and $\sigma_c = 815$ MPa, $h_c = 0.18$, $\varepsilon_c = 0.25$, $b = -0.114$ and $c = -0.54$. The best FCG curve fitted to this material is slightly more complex [19], $da/dN = 5 \times 10^{-10} \cdot (\Delta K - \Delta K_{th})^2 \cdot \{K_c/[K_c - \Delta K/(1 - R)]\}$, where $\Delta K_{th} = 11.6$ and $K_c = 277$ (ΔK, ΔK_{th} and K_c in MPa $\sqrt{m}$ and da/dN in m/cycle).

The VA load history in this case is a series of blocks containing 101 peaks and valleys each, as shown in Fig. 10. Once again a high mean R-ratio is used in this test, to avoid the interference of possible significant closure effects which could mask the model performance. The predictions using the proposed algorithm are compared with the measured crack propagation data in Fig. 11. These predictions are again quite reasonable, in special when ΔK_{th} is considered in the algorithm. Therefore, one can claim that these tests indicate that the ideas behind the proposed critical damage model make sense and deserve to be better explored.

7. Conclusions

A damage accumulation model ahead of the crack tip, based on εN cyclic properties, was presented to predict fatigue crack propagation under variable amplitude loading. The model treats the crack as a sharp notch with a small but finite radius to avoid singularity problems, and calculates damage accumulation explicitly at each load cycle. An algorithm was proposed to efficiently evaluate crack growth under variable amplitude loading from strain-life data. Experimental results show a good agreement between measured crack growth, both under constant and variable amplitude loading, and the predictions based purely on εN data.

References

[1] S. Majumdar, J. Morrow, ASTM STP 559 (1974) 159–182.
[2] J.A.R. Durán, J.T.P. Castro, J.C. Payão Filho, FFEMS 26 (2003) 137–150.
[3] S. Suresh, Fatigue of Materials, second ed., Cambridge, 1998.
[4] M. Skorupa, FFEMS 21 (1998) 987–1106.
[5] M. Skorupa, FFEMS 22 (1999) 905–926.
[6] J.T.P. Castro, M.A. Meggiolaro, A.C.O. Miranda, Int. J. Fatigue 27 (2005) 1366–1388.
[7] A.K. Vasudevan, K. Sadananda, R.L. Holtz, Int. J. Fatigue 27 (2005) 1519–1529.
[8] M.A. Meggiolaro, J.T.P. Castro, Int. J. Fatigue 25 (2003) 843–854.

[9] K.H. Schwalbe, Eng. Fract. Mech. 6 (1974) 325–341.
[10] G. Glinka, Eng. Fract. Mech. 21 (1985) 245–261.
[11] D. Kujawski, F. Ellyin, Int. J. Fatigue 6 (1984) 83–87.
[12] D. Kujawski, F. Ellyin, Fract. Mech. 28; (1987) 367–378.
[13] M. Creager, P.C. Paris, Int. J. Fract. Mech. 3 (1967) 247–252.
[14] H. Neuber, J. Appl. Mech. 28 (1961) 544–551.
[15] K. Molsky, G. Glinka, Mater. Sci. Eng. 50 (1981) 93–100.
[16] R. Stephens, A. Fatemi, R.R. Stephens, H.O. Fuchs, Metal Fatigue in Engineering, Interscience, 2000.
[17] Webpage <www.tecgraf.puc-rio.br/vida>, 2009, (last accessed 02.09).
[18] V.Z. Parton, E.M. Morozov, Elastic–Plastic Fracture Mechanics, Mir Publishers, 1978.
[19] J.T.P. Castro, M.A. Meggiolaro, Fadiga sob Cargas Reais de Serviço, Livro Técnico Científico ed., Brazil, 2009 (in Portuguese).
[20] M. Mazari, B. Bouchouicha, M. Zemri, M. Benguediab, N. Ranganathan, Comput. Mater. Sci. 41 (2008) 344–349.
[21] J.A.R. Durán, M.G. Souza, J.T.P. Castro, M.A. Meggiolaro, Crack growth predictions under variable amplitude loading based on low cycle fatigue data, in: Fifth International Conference on Low Cycle Fatigue, Berlin, Germany, 2003.
[22] J.A.R. Durán, J.T.P. Castro, M.A. Meggiolaro, A Damage Accumulation Model to Predict Fatigue Crack Growth Under Variable Amplitude Loading Using εN Parameters, in Fatigue v.4, EMAS, UK, 2002, pp. 2759–2776.